

RESEARCH ARTICLE | JUNE 02 2021

Single photon emission from ODT passivated near-surface GaAs quantum dots

Special Collection: [Non-Classical Light Emitters and Single-Photon Detectors](#)

Xin Cao ; Jingzhong Yang ; Pengji Li; Yiteng Zhang; Eddy P. Rugeramigabo; Benedikt Brechtken; Rolf J. Haug ; Michael Zopf ; Fei Ding

Check for updates

Appl. Phys. Lett. 118, 221107 (2021)

<https://doi.org/10.1063/5.0046042>



CrossMark

Boost Your Optics and Photonics Measurements

Lock-in Amplifier

Zurich Instruments

[Find out more](#)

Boxcar Averager

Single photon emission from ODT passivated near-surface GaAs quantum dots

Cite as: Appl. Phys. Lett. **118**, 221107 (2021); doi: [10.1063/5.0046042](https://doi.org/10.1063/5.0046042)

Submitted: 31 January 2021 · Accepted: 12 May 2021 ·

Published Online: 2 June 2021



View Online



Export Citation



CrossMark

Xin Cao,¹ Jingzhong Yang,¹ Pengji Li,¹ Yiteng Zhang,¹ Eddy P. Rugeramigabo,¹ Benedikt Brechtken,¹ Rolf J. Haug,^{1,2} Michael Zopf,^{1,a)} and Fei Ding^{1,2,a)}

AFFILIATIONS

¹Institut für Festkörperphysik, Leibniz Universität Hannover, Appelstraße 2, 30167 Hannover, Germany

²Laboratorium für Nano- und Quantenengineering, Leibniz Universität Hannover, Schneiderberg 39, 30167 Hannover, Germany

Note: This paper is part of the APL Special Collection on Non-Classical Light Emitters and Single-Photon Detectors.

^{a)}Authors to whom correspondence should be addressed: zopf@fkp.uni-hannover.de and f.ding@fkp.uni-hannover.de

ABSTRACT

Epitaxially grown semiconductor quantum dots are promising candidates for pure single photon and polarization-entangled photon pair emission. Excellent optical properties can typically be ensured only if these so-called “artificial atoms” are buried deep inside the semiconductor host material. Quantum dots grown close to the surface are prone to charge carrier fluctuations and trap states on the surface, degrading the brightness, coherence, and stability of the emission. We report on high-purity single photon emission [$g^{(2)}(0) = 0.016 \pm 0.015$] of GaAs/AlGaAs quantum dots that were grown only 20 nm below the surface. Chemical surface passivation with sulfur compounds such as octadecanethiol has been performed on quantum dots with 20, 40, and 98 nm from the surface. The reduction of the density and influence of surface states causes improvements in linewidth and photoluminescence intensity as well as a well-preserved single photon emission. Therefore, the realization of hybrid nanophotonic devices, comprising near-field coupling and high-quality optical properties, comes into reach.

© 2021 Author(s). All article content, except where otherwise noted, is licensed under a Creative Commons Attribution (CC BY) license (<http://creativecommons.org/licenses/by/4.0/>). <https://doi.org/10.1063/5.0046042>

Single photon and entangled photon sources are key components for quantum communication,^{1,2} optical quantum computing,^{3,4} and quantum metrology.⁵ Many types of quantum light source have been developed in the past few decades, based on spontaneous parametric downconversion (SPDC),^{6,7} epitaxial quantum dots (QDs),^{8–10} defects in diamond,^{11,12} or silicon carbide,¹³ to name only a few. SPDC sources are the main workhorse of the present quantum communication and have been implemented in first field-tests of satellite-based intercontinental quantum key distribution.¹⁴ Epitaxially grown semiconductor quantum dots are considered as the next most promising candidate due to many advantages: on-demand photon emission, ultrahigh single photon purity¹⁵ and indistinguishability,⁹ wide wavelength tunability,¹⁶ both optical and electrical excitation,¹⁷ and compatibility with state-of-the-art semiconductor technology.¹⁸ Defect centers in diamond are mainly used in quantum metrology, thanks to their long spin coherence times,¹⁹ while other types of defects such as in silicon carbide are also being studied.

Widely used material systems for epitaxial quantum dots include GaAs/AlGaAs,¹⁰ InAs/GaAs,²⁰ InAs/InP,²¹ and GaN/AlGaIn,²² by which emission of photons from the ultraviolet to the near infrared region can be achieved. However, all these quantum dots are typically

deeply buried inside the host matrix, more than 100 nm away from the surface. The research efforts in the past three decades have led to well-developed sample growth techniques as well as advanced micro- and nanofabrication methods. Hybrid nanophotonic devices with near-field coupling can, therefore, be investigated, such as QDs coupled with surface plasmons²³ or a single photon transistor.²⁴ Since surface plasmon coupling requires a very small distance (<25 nm) between the plasmon and the emitter,²⁵ near surface QDs are demanded for such applications.

The optical properties of semiconductor micro- and nanostructures are greatly affected by their surface. Defects in the crystal lattice usually result in additional electronic states in the bandgap (so-called surface states), which is detrimental for radiative recombination processes and charge carrier transport. The past research and technological advance of optoelectronic devices based on gallium arsenide, therefore, kindled an interest in surface passivation.^{26–28} It is known that oxygen and dangling bonds at the GaAs surface lead to additional recombination channels and result in scattering of charge carriers.²⁹ An increase in photoluminescence (PL) intensity by more than one order of magnitude has been observed after passivating the GaAs surface with sulfur.³⁰ Nonradiative recombination processes are

suppressed because the surface atoms covalently bind with sulfur, thereby forming harder states.²⁸ However, all these studies are on GaAs bulk material, one study reports on surface passivation on GaAs QDs.³¹ Up to now, although some groups worked on InAs or InGaAs QDs directly at the surface, all the obtained photoluminescence signals were from an ensemble of QDs and no single surface QD emission has been observed.^{32,33} Heyn and co-workers studied GaAs QDs with reduced capping layer thickness, but the linewidth of the single photon emission lines increased significantly.³⁴ Manna and co-workers grew GaAs QDs with thick capping layers and reduced the capping thickness with chemical etching afterwards. Then they used ammonia sulfide to passivate the surface and deposited a dielectric alumina overlayer for protection, which led to a partial restoration of the linewidth of the near surface single GaAs QD. However, the final capping layer thickness was increased to 42–48 nm after the alumina over-layer deposition.³¹

In this work, we investigate the linewidth broadening and fluorescence quenching by reducing the capping layer thickness from 98 to 20 nm. We passivate the surface using octadecanethiol (ODT), a treatment that is applicable for many III–V material systems, such as InP,³⁵ GaN,³⁶ and GaSb.³⁷ The linewidth and intensity are partially restored, and single photon emission of the GaAs QDs is still preserved even with 20 nm capping. Bunching effects in the second-order intensity autocorrelation measurements are alleviated after ODT passivation, indicating the elimination of additional states and decay channels at the surface.

The QD sample is grown on an undoped GaAs (001) substrate (Wafer Technology Ltd.) with solid source molecular beam epitaxy (MBE, Riber, Compact 21) via the local droplet etching method.³⁸ First, the substrate is deoxidized and overgrown with a GaAs buffer at a temperature of 620 °C. After that, AlGaAs is deposited as a base for the subsequent QD growth. After interrupting As₄ for a short period to create a low arsenic environment, Al droplets are deposited on the AlGaAs surface. Due to the atomic concentration gradients between the surface layer and the Al droplets, interdiffusion of As and Al takes place, resulting in the formation of symmetric nanoholes on the surface.³⁹ By supplying Ga and As₄, GaAs forms at the surface, which then migrates into the nanoholes to minimize the surface energy. After that, the QDs are capped with AlGaAs again with a thickness of 98, 40, and 20 nm, respectively, as shown in Fig. 1(a).

The surface morphology of the as-grown samples is investigated with an atomic force microscope (AFM, Veeco, NanoScope V) as shown in Figs. 1(b)–1(d). The surface is smooth (rms < 0.2 nm), and the density of the QDs is in the range of 0.1 μm^{-2} , which is consistent with previous reports.¹⁶ With 20 nm capping thickness over the QD, the nanohole morphology is still preserved, indicating that the nanoholes are partially infilled by the GaAs QDs [Fig. 1(b)]. When the AlGaAs capping is increased to 40 nm, the dips can be hardly seen, and larger bumps remain on the surface with 98 nm capping. This effect is caused by the capillary force of the nanoholes and surface reconstruction. The ability to observe the QD location even with larger capping thicknesses is an advantage for the realization of hybrid nanophotonic devices: The position of nanostructures (e.g., plasmonic nanoparticles) can therefore be manipulated with the AFM and the position on top of the QD precisely adjusted, without any need for optical measurement.

After sample growth, the samples are cut into pieces. Chemical treatment is performed by immersing the sample pieces in 0.05 mol/l

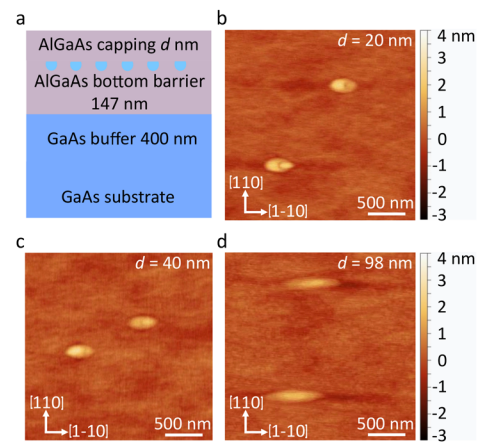


FIG. 1. (a) Schematic of the sample structure. (b)–(d) AFM images of GaAs QDs with a capping layer thickness of $d = 20, 40, 98$ nm, respectively. The elevated structures on the surface indicate the location of the nanoholes below the capping layer.

1-Octadecanethiol (ODT, Sigma-Aldrich)/ethanol (Carl Roth GmbH) for 3 h to passivate the surface. The following optical measurements were performed at 4 K by inserting the different pieces of sample (with and without passivation) into a closed-cycle helium flow cryostat (Montana Instruments, Cryostation C2). Single QDs are excited using continuous wave diode laser at 675 nm (Thorlabs) which is focused by an objective (MicroscopeWorld, M Plan Apo NIR 100 \times) with a numerical aperture of 0.7 before irradiating the sample.

The low density of the QDs allow us to probe individual QDs. Figure 2 displays the micro-photoluminescence (PL) spectra of GaAs QDs with three capping thicknesses, before and after ODT passivation, obtained under an excitation laser power of 550 nW. It clearly shows the dominant neutral exciton peak and several charged exciton peaks at the redshifted side. By reducing the capping thickness, the intensity of the exciton peaks of the as-grown sample is significantly decreased and the linewidth is broadened. This indicates the presence of extra decay channels caused by surface states as well as the influence of electric fields from the charge carrier fluctuations at the surface via the DC Stark effect. After ODT passivation, it is difficult to observe any change from the PL spectra for the sample with 98 nm capping. For 40 and 20 nm, the intensity of the exciton emission is enhanced after passivation. Even at a low capping thickness of 20 nm, the different excitonic peaks can be clearly resolved.

To further illustrate the influence of surface passivation on the neutral exciton, a double stage spectrometer with a focal length of 750 mm for each stage (Spectroscopy & Imaging GmbH) is used to characterize the linewidth with high resolution, as shown in Fig. 3. By reducing the capping thickness from 98 to 20 nm, the linewidth shows about sixfold broadening. With 98 nm capping, the linewidth of the neutral exciton is limited by the spectrometer resolution (about 20 μeV). Both the linewidth and PL intensity do not change after passivation [Figs. 4(a) and 4(b)] since the QDs are deeply buried inside the AlGaAs matrix, beyond the influence of the surface states. For 40 nm capping, the surface states start to affect the exciton recombination (linewidth of about 48 μeV). When further reducing the capping thickness to 20 nm, the peak shows an additional threefold broadening

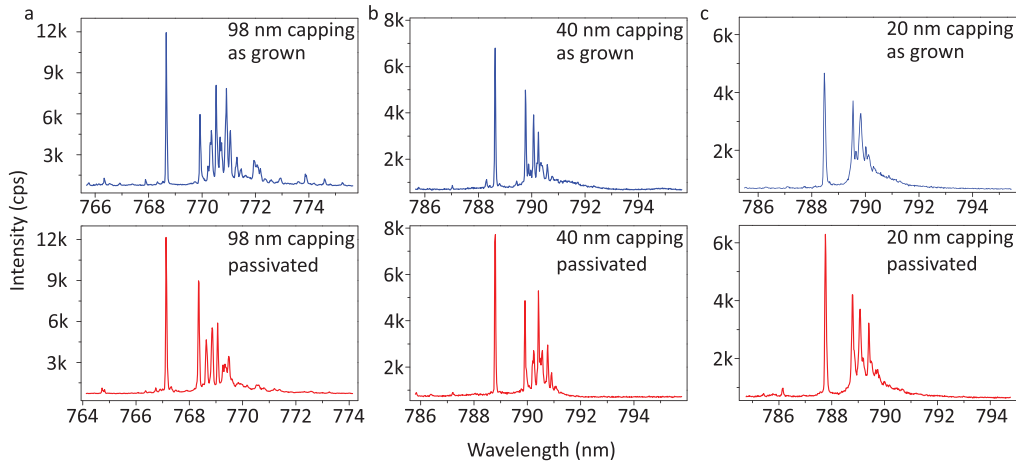


FIG. 2. PL spectra of different GaAs QDs representing the average emission of each sample before and after passivation for different capping thicknesses. Top: as grown sample; bottom: passivated sample. Linewidth and intensities decrease with lower capping thickness. These properties are partially restored after surface passivation.

compared with 40 nm capping. This can be explained by two mechanisms. On the one hand, due to the abrupt end of the crystal lattice at the surface, charge carriers may accumulate at the surface and will occupy and de-occupy surface states. Such moving charge carriers will result in a fluctuating electric field and therefore affect the exciton emission energy on short timescales (typically $< \text{ms}$) due to the DC Stark effect, causing peak broadening on longer timescales ($> \text{ms}$). When the QD is closer to the surface, the stronger electric field fluctuations will induce larger peak broadening. On the other hand, AlGaAs is easily oxidized in air. The oxides will result in additional charge carrier trap states, leading to an increase in nonradiative transitions of the exciton, which is described by

$$\frac{1}{\tau} = A_{21} + \frac{1}{\tau_{NR}}, \quad (1)$$

where τ is lifetime of the exciton, A_{21} is the Einstein coefficient, and τ_{NR} is the nonradiative relaxation time. According to Eq. (1), the nonradiative relaxation time shortens the lifetime of the exciton emission, thus broadening the exciton peak. However, after ODT treatment sulfur can partially replace the oxides,⁴⁰ decreasing the trap state density.

Since sulfur forms covalent bonds with surface atoms resulting in the formation of harder states, nonradiative recombination processes are reduced,²⁸ and the radiative lifetime of the exciton can be partially restored. Studying an average of 30 dots reveals a reduction of the linewidth of the 40 and 20 nm capping samples by 8 and 25 μeV , respectively, after ODT passivation [Figs. 3(b), 3(c), and 4(a)]. The intensity of the neutral exciton emission is also enhanced [Fig. 4(b)] as the passivation reduces nonradiative transitions.

Buried GaAs QDs have proven to be ultrapure single photon sources.¹⁵ Owing to the limited number of studies on near surface QDs, single photon emission behavior has not been reported before. Figures 4(c) and 4(d) show the second-order autocorrelation measurement of the as grown and passivated sample with 20 nm capping. Hereby, the single photon emission is detected using avalanche photodiodes (APD, Laser Components) with a time resolution of 350 ps. The coincidence histogram is fitted with the following correlation function, convoluted with the instrument response function of the APD:

$$g^{(2)}(\tau) = \left(1 + \frac{1 - \beta}{\beta} e^{-\frac{|\tau|}{\tau_c}} \right) g_{ideal}^{(2)}(\tau), \quad (2)$$

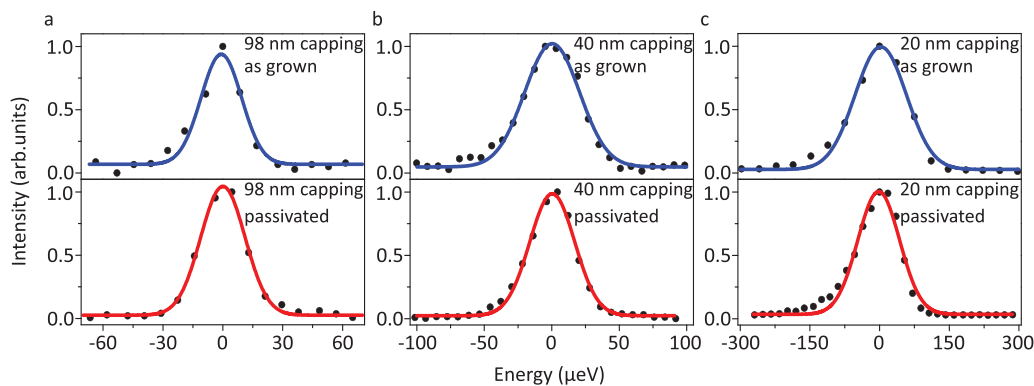


FIG. 3. Typical linewidth of neutral exciton peak of different samples before and after passivation. The peaks are fitted with a Gaussian line shape.

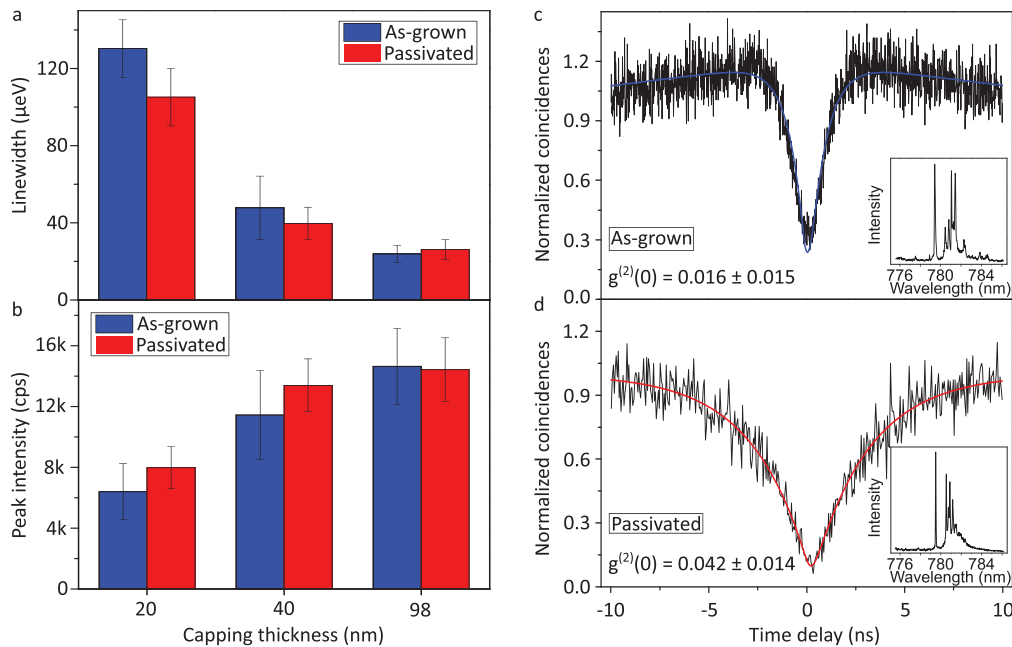


FIG. 4. Left panel: comparison of linewidth (a) and saturated peak intensity (b) of the neutral exciton emission from GaAs near-surface QD samples before and after passivation. 30, 30, and 29 quantum dots were measured for 20, 40, and 98 nm capping thickness, respectively. The linewidth is 23.9/26.1 μeV for 98 nm capping, 47.8/39.6 μeV for 40 nm capping and 130.3/105.1 μeV for 20 nm capping for the as grown/passivated samples, respectively. The peak intensity is measured at saturated excitation power of 1.6 μW . Right panel: second-order autocorrelation measurement of as grown (c) and passivated (d) sample with 20 nm capping. The anti-bunching dip at zero-time delay indicates single photon emission, with $g^{(2)}(0) = 0.016 \pm 0.015$ and 0.042 ± 0.014 for as grown and passivated, respectively. Slight bunching for the as-grown sample is attributed to the blinking effect, which is not present after ODT passivation. Surface passivation also reduces nonradiative transitions, resulting in the broadening of the anti-bunching dip. Inset: PL spectra of the measured QDs.

$$g_{\text{ideal}}^{(2)}(\tau) = (g_0 - 1)e^{-\frac{|\tau|}{\tau_{\text{corr}}}} + 1, \quad (3)$$

where τ_c corresponds to the correlation time of the characteristic blinking effect, τ_{corr} is the characteristic correlation timescale, β is the fraction of time when the QD is in an “on” state, and g_0 is the $g^{(2)}$ value at time = 0.^{41,42} Both samples are pure single photon emitters, proven by the low values of $g^{(2)}(0) = 0.016 \pm 0.015$ and 0.042 ± 0.014 , respectively. These values have not been corrected for detector dark counts. The autocorrelation measurement on the as grown sample shows a slight bunching effect. This is attributed to blinking in the exciton emission induced by trap states. After ODT passivation, the bunching effect is not observed, indicating a reduction of the density of trap states. In addition, the anti-bunching dip is broadened after ODT passivation. On the one hand, this is a clear indication that the nonradiative transition channels have been reduced, and the lifetime of the exciton is prolonged, consistent with the previous linewidth measurements. On the other hand, the passivation may lead to a stronger phonon bottleneck in the QDs⁴³ since excited exciton recombination dynamics can be affected by surface states. Broadening of the anti-bunching dip can then be attributed to slower excited exciton relaxation. This also enhances hot luminescence processes, which is observed for the passivated sample [Fig. 2(c)] where higher-energetic spectral features become slightly more prominent.

In conclusion, we have shown that the quantum dot emission is not influenced by surface states when the dots are buried around 100 nm beneath the surface. By reducing the quantum dot to surface

distance from 40 to 20 nm, surface states have stronger influence on the QD emission. The addition of nonradiative decay channels and charge fluctuations results in linewidth broadening and fluorescence quenching. By applying chemical passivation with ODT, the surface states are partially eliminated, inducing a partial recovery of linewidth and intensity. The single photon emission properties and excitonic spectral features are very well preserved even for 20 nm capping. The presence of blinking in the single photon emission is reduced with ODT passivation. The passivation of near surface quantum dots paves the way for hybrid nanophotonic devices where near-field coupling is needed, such as surface plasmon coupling. Although ODT can partially passivate the surface states, the surface states cannot be totally eliminated, which motivates the investigation of more efficient methods for complete passivation of the semiconductor surface. Applying more reactive sulfur compounds such as $(\text{NH}_4)_2\text{S}_x$ may yield better passivation.⁴⁰

AUTHORS' CONTRIBUTIONS

X.C., J.Y., and P.L. contributed equally to this work.

The authors thank Zhao An for fruitful discussion. The authors gratefully acknowledge the funding by the German Federal Ministry of Education and Research (BMBF) within the project Q.Link.X (No. 16KIS0869), the funding by the European Research Council (No. QD-NOMS GA715770), and the Deutsche

Forschungsgemeinschaft (DFG, German Research Foundation) under Germany's Excellence Strategy-EXC-2123 Quantum Frontiers-390837967.

DATA AVAILABILITY

The data that support the findings of this study are available from the corresponding authors upon reasonable request.

REFERENCES

- ¹J. Yin, J. Ren, H. Lu, Y. Cao, H. Yong, Y. Wu, C. Liu, S. Liao, F. Zhou, Y. Jiang, X. Cai, P. Xu, G. Pan, J. Jia, Y. Huang, H. Yin, J. Wang, Y. Chen, C. Peng, and J. Pan, *Nature* **488**, 185 (2012).
- ²S. K. Liao, H. L. Yong, C. Liu, G. L. Shentu, D. D. Li, J. Lin, H. Dai, S. Q. Zhao, B. Li, J. Y. Guan, W. Chen, Y. H. Gong, Y. Li, Z. H. Lin, G. S. Pan, J. S. Pelc, M. M. Fejer, W. Z. Zhang, W. Y. Liu, J. Yin, J. G. Ren, X. Bin Wang, Q. Zhang, C. Z. Peng, and J. W. Pan, *Nat. Photonics* **11**, 509 (2017).
- ³E. Knill, R. Laflamme, and G. J. Milburn, *Nature* **409**, 46 (2001).
- ⁴H.-S. Zhong, H. Wang, Y.-H. Deng, M.-C. Chen, L.-C. Peng, Y.-H. Luo, J. Qin, D. Wu, X. Ding, Y. Hu, P. Hu, X.-Y. Yang, W.-J. Zhang, H. Li, Y. Li, X. Jiang, L. Gan, G. Yang, L. You, Z. Wang, L. Li, N.-L. Liu, C.-Y. Lu, and J.-W. Pan, *Science* **370**, 1460 (2020).
- ⁵M. A. Taylor and W. P. Bowen, *Phys. Rep.* **615**, 1 (2016).
- ⁶D. C. Burnham and D. L. Weinberg, *Phys. Rev. Lett.* **25**, 84 (1970).
- ⁷P. G. Kwiat, K. Mattle, H. Weinfurter, A. Zeilinger, A. V. Sergienko, and Y. Shih, *Phys. Rev. Lett.* **75**, 4337 (1995).
- ⁸O. Benson, C. Santori, M. Pelton, and Y. Yamamoto, *Phys. Rev. Lett.* **84**, 2513 (2000).
- ⁹X. Ding, Y. He, Z. C. Duan, N. Gregersen, M. C. Chen, S. Unsleber, S. Maier, C. Schneider, M. Kamp, S. Höfling, C. Y. Lu, and J. W. Pan, *Phys. Rev. Lett.* **116**, 020401 (2016).
- ¹⁰R. Keil, M. Zopf, Y. Chen, B. Höfer, J. Zhang, F. Ding, and O. G. Schmidt, *Nat. Commun.* **8**, 15501 (2017).
- ¹¹L. Childress and R. Hanson, *MRS Bull.* **38**, 134 (2013).
- ¹²E. Neu, D. Steinmetz, J. Riedrich-Möller, S. Gsell, M. Fischer, M. Schreck, and C. Becher, *New J. Phys.* **13**, 025012 (2011).
- ¹³J. Wang, Y. Zhou, Z. Wang, A. Rasmita, J. Yang, X. Li, H. J. von Bardeleben, and W. Gao, *Nat. Commun.* **9**, 4106 (2018).
- ¹⁴S. Liao, W. Cai, J. Handsteiner, B. Liu, J. Yin, L. Zhang, D. Rauch, M. Fink, J. Ren, W. Liu, Y. Li, Q. Shen, Y. Cao, F. Li, J. Wang, Y. Huang, L. Deng, T. Xi, L. Ma, T. Hu, L. Li, N. Liu, F. Koidl, P. Wang, Y. Chen, X. Wang, M. Steindorfer, G. Kirchner, C. Lu, R. Shu, R. Ursin, T. Scheidl, C. Peng, J. Wang, A. Zeilinger, and J. Pan, *Phys. Rev. Lett.* **120**, 030501 (2018).
- ¹⁵L. Schweickert, K. D. Jöns, K. D. Zeuner, S. F. Covre Da Silva, H. Huang, T. Lettner, M. Reindl, J. Zichi, R. Trotta, A. Rastelli, and V. Zwiller, *Appl. Phys. Lett.* **112**, 093106 (2018).
- ¹⁶P. Atkinson, E. Zallo, and O. G. Schmidt, *J. Appl. Phys.* **112**, 054303 (2012).
- ¹⁷J. Zhang, J. S. Wildmann, F. Ding, R. Trotta, Y. Huo, E. Zallo, D. Huber, A. Rastelli, and O. G. Schmidt, *Nat. Commun.* **6**, 10067 (2015).
- ¹⁸J. H. Kim, S. Aghaieimebodi, C. J. K. Richardson, R. P. Leavitt, D. Englund, and E. Waks, *Nano Lett.* **17**, 7394 (2017).
- ¹⁹G. Balasubramanian, P. Neumann, D. Twitchen, M. Markham, R. Kolesov, N. Mizuochi, J. Isoya, J. Achard, J. Beck, J. Tessler, V. Jacques, P. R. Hemmer, F. Jelezko, and J. Wrachtrup, *Nat. Mater.* **8**, 383 (2009).
- ²⁰C. Carmesin, F. Olbrich, T. Mehrtens, M. Florian, S. Michael, S. Schreier, C. Nawrath, M. Paul, J. Höschele, B. Gerken, J. Kettler, S. L. Portalupi, M. Jetter, P. Michler, A. Rosenauer, and F. Jahnke, *Phys. Rev. B* **98**, 125407 (2018).
- ²¹A. Musiał, P. Holewa, P. Wyborski, M. Syperek, A. Kors, J. P. Reithmaier, G. Sek, and M. Benyoucef, *Adv. Quantum Technol.* **3**, 1900082 (2020).
- ²²M. Arita, F. L. Roux, M. J. Holmes, S. Kako, and Y. Arakawa, *Nano Lett.* **17**, 2902 (2017).
- ²³M. Pfeiffer, P. Atkinson, A. Rastelli, O. G. Schmidt, H. Giessen, M. Lippitz, and K. Lindfors, *Sci. Rep.* **8**, 3415 (2018).
- ²⁴D. E. Chang, A. S. Sorensen, E. A. Demler, and M. D. Lukin, *Nat. Phys.* **3**, 807 (2007).
- ²⁵A. Regler, K. Schraml, A. Lyamkina, M. Spiegel, K. Müller, J. Vuckovic, J. J. Finley, and M. Kaniber, *J. Nanophotonics* **10**, 033509 (2016).
- ²⁶C. J. Sandroff, M. S. Hegde, L. A. Farrow, C. C. Chang, and J. P. Harbison, *Appl. Phys. Lett.* **54**, 362 (1989).
- ²⁷T. Ohno, *Phys. Rev. B* **44**, 6306 (1991).
- ²⁸V. N. Bessolov, E. V. Konenkova, and M. V. Lebedev, *J. Vac. Sci. Technol. B* **14**, 2761 (1996).
- ²⁹C. J. Spindt and W. E. Spicer, *Appl. Phys. Lett.* **55**, 1653 (1989).
- ³⁰H. A. Budz and R. R. LaPierre, *J. Vac. Sci. Technol. A* **26**, 1425 (2008).
- ³¹S. Manna, H. Huang, S. F. C. da Silva, C. Schimpf, M. B. Rota, B. Lehner, M. Reindl, R. Trotta, and A. Rastelli, *Appl. Surf. Sci.* **532**, 147360 (2020).
- ³²Q. Yuan, B. Liang, C. Zhou, Y. Wang, Y. Guo, S. Wang, G. Fu, Y. I. Mazur, M. E. Ware, and G. J. Salamo, *Nanoscale Res. Lett.* **13**, 387 (2018).
- ³³G. Wang, B. Liang, B. Juang, A. Das, M. C. Debnath, D. L. Huffaker, Y. I. Mazur, M. E. Ware, and G. J. Salamo, *Nanotechnology* **27**, 465701 (2016).
- ³⁴C. Heyn, M. Zocher, L. Pudewill, H. Runge, A. Künster, and W. Hansen, *J. Appl. Phys.* **121**, 044306 (2017).
- ³⁵M. Schvartzman, V. Sidorov, D. Ritter, and Y. Paz, *Semicond. Sci. Technol.* **16**, L68 (2001).
- ³⁶C. Zhao, T. K. Ng, A. Prabaswara, M. Conroy, S. Jahangir, T. Frost, J. O'Connell, J. D. Holmes, P. J. Parbrook, P. Bhattacharya, and B. S. Ooi, *Nanoscale* **7**, 16658 (2015).
- ³⁷E. Papis-Polakowska, J. Kaniewski, J. Jureczyk, A. Jasik, K. Czuba, A. E. Walkiewicz, and J. Szade, *AIP Adv.* **6**, 055206 (2016).
- ³⁸Z. M. Wang, B. L. Liang, K. A. Sablon, and G. J. Salamo, *Appl. Phys. Lett.* **90**, 113120 (2007).
- ³⁹C. Heyn, S. Schnüll, and W. Hansen, *J. Appl. Phys.* **115**, 024309 (2014).
- ⁴⁰Y. Nannichi, J.-F. Fan, H. Oigawa, and A. Koma, *Jpn. J. Appl. Phys., Part 2* **27**, L2367 (1988).
- ⁴¹J. P. Jahn, M. Munsch, L. Béguin, A. V. Kuhlmann, M. Renggli, Y. Huo, F. Ding, R. Trotta, M. Reindl, O. G. Schmidt, A. Rastelli, P. Treutlein, and R. J. Warburton, *Phys. Rev. B* **92**, 245439 (2015).
- ⁴²C. Hopfmann, N. L. Sharma, W. Nie, R. Keil, F. Ding, and O. G. Schmidt, *arXiv:2011.14641v1* (2020).
- ⁴³R. Heitz, H. Born, F. Guffarth, O. Stier, A. Schliwa, A. Hoffmann, and D. Bimberg, *Phys. Rev. B* **64**, 241305 (2001).